HHS Public Access

Author manuscript

Magn Reson Med. Author manuscript; available in PMC 2018 July 01.

Published in final edited form as:

Magn Reson Med. 2017 July ; 78(1): 383–386. doi:10.1002/mrm.26344.

Potential for High-Permittivity Materials to Reduce Local SAR at a Pacemaker Lead Tip During MRI of the Head With a Body Transmit Coil at 3T

Zidan Yu[1], **Xuegang Xin**[2], and **Christopher M. Collins**[1,*]

[1]Department of Radiology, New York University College of Medicine, New York, NY, USA

[2]Provincial Key Laboratory of Medical Image Processing, Southern Medical University, Guang Zhou, Guang Dong Province, China

Abstract

Purpose—Illustrate potential for high permittivity materials to be used in decreasing peak local SAR associated with implants when the imaging region is far from the implant.

Methods—Numerical simulations of a human subject with a pacemaker in a body-sized birdcage coil driven at 128MHz with and without a thin (5mm) shell of material of high electric permittivity around the head were performed.

Results—For a shell with relative permittivity of 600, the maximum Specific energy Absorption Rate (SAR) averaged over any 1g of tissue near the pacemaker was reduced by 73.5% for a given B_1 field strength at the center of brain.

Conclusion—While significant further work is required, initial simulations indicate that strategic use of high permittivity materials may broaden the conditions under which patients containing some implants can be imaged safely.

Keywords

MRI; dielectric; permittivity; pacemaker; safety

Introduction

Due to increases in both usage of MRI in medical practice and the number of patients with implantable cardiovascular devices, the likelihood for a patient being indicated for an MRI over the lifetime of their device is as high as 75% (1). Unfortunately, the presence of most types of pacemakers in use today is a contraindication to MRI due to potential hazards ranging from device malfunction to direct tissue damage (2). One of the most significant risks is that of strong deposition of radiofrequency (RF) energy, or specific absorption rate (SAR), at the tip of the pacemaker lead: RF currents induced in the lead wire can be

*Address correspondence to: Christopher M. Collins, PhD, 660 First Ave, Fourth Floor, Room 403, New York, NY 10016, c.collins@nyumc.org, (212)263-3322.

deposited in the tissue at the point where the lead is connected to the cardiac tissue, resulting in excessive heating there (3).

Although the FDA approved the first magnetic resonance conditional pacemaker system (SURESCAN) in 2011, limitations still exist (4). For example, there is still a need for performing MRI on patients who rely on other pacemakers, and the approved conditions under which a patient with the SURESCAN device can be imaged are limited to 1.5T MRI systems, which have relatively low RF power levels for a given MRI sequence when compared to power required at higher field strengths. In practice, the vast majority of clinical MRI exams are performed with a whole-body transmit coil rather than a local transmit coil, and head-only transmit coils are not currently available at all sites.

Previous studies have shown with simulation and experiment that in MRI at 3T, strategic placement of high permittivity materials around the region of interest (ROI) has the potential to, among other things, enhance the strength of the RF magnetic (B_1) field in that region relative to others, allowing for reduced overall input power and reducing whole-body SAR for a desired B_1 field strength in the ROI (5–10).

To explore the possibility of reducing local tissue heating related to a pacemaker in MRI with strategic use of high permittivity materials, we performed numerical simulations including a thin shell of high permittivity material surrounding the head of a patient wearing pacemaker during RF excitation of the head at 3T with use of a whole-body transmit coil. We then selected an optimal relative permittivity for the material surrounding the head, considering both the homogeneity of the B_1 field in the brain and SAR at the lead tip, and examined the resulting field and SAR distributions.

Methods

A resonant 16-element birdcage coil (76-cm diameter, 65-cm length, with a shield 84-cm in diameter and 90-cm in length) was modeled, tuned to 128MHz, and driven with two sources in quadrature (2 sources 90 apart in azimuthal location and phase of the driving voltage source). This geometry is representative of realistic body-sized birdcage coils, and coils of similar dimensions would be expected to produce similar results. A 3D adult human body model, “Duke,” (11) with 2mm anatomical resolution was placed with the brain at the center of the birdcage coil. The appropriate values of tissue mass density and electrical properties at 128MHz were assigned to the human model. A bipolar-lead pacemaker model was created within the human model with the housing beneath the upper chest skin. The lead (1.4-mm diameter metal core coated with 1mm thick silicone rubber layer) went through the subclavean vein, ending at the bottom of the right ventricle with the lead tip in contact with the cardiac muscle. The pacemaker lead was insulated everywhere but at the tip. A 5mm-thick layer of high permittivity material, conformal with the shape of the head, was placed around the head of the human model. The simulation geometry used in this study is shown in Figure 1.

All field calculations were performed with numerical methods using SEMCAD-X software (Schmidt & Partner Engineering AG, Zürich, Switzerland), and post-processing of the

simulation results was performed with in-house code on a MATLAB platform (The Mathworks, Inc., Natick, MA). The relative permittivity of the high-dielectric shell was varied from 1 to 900 and the homogeneity of the B_1 field in the brain and the 1g peak special-average SAR of the tissue around the implanted lead tip was evaluated for each case. The coefficient of Variation (standard deviation divided by average) was used to characterize homogeneity of the B_1^+ field on the mid-axial slice through the brain. To compare the SAR deposition around the lead tip with different helmet dielectric properties, the maximum peak SAR around the lead tip was normalized by the square of the B_1^+ amplitude at the center of the brain. For the case with optimal performance, additional simulations and analyses were conducted with realistic electrical conductivities assigned to the high permittivity material.

Results

The upper portion of Figure 2 shows the B_1^+ field distribution on a coronal plane through the middle of the coil, normalized to have the same average field strength in the brain. The effect of the high permittivity material enhancing the fields in the brain results in lower required input power to maintain the desired field strength in brain and weaker fields outside the brain when the high permittivity material is present. Table 1 shows the results of permittivity on peak SAR at the lead tip normalized to B_1^+ strength in the brain (Peak SAR/|B1+|^2) and B_1^+ homogeneity (Coefficient of Variation of $|B_1^+|$) in the brain. Considering both these factors, we selected a relative electric permittivity (ε_r) of 600 for the high permittivity material. The transmit efficiency (B_1^+ in brain divided by the square root of power dissipated in the entire body) with this high permittivity material present is 54% better than when it is absent. The lower portion of Figure 2 shows the distribution of 1g average SAR on a transverse plane containing the pacemaker lead tip with the coil driven to produce the same average B_1^+ field strength both with and without the high permittivity material present. The normalized peak SAR around the lead tip is 73.5% lower with the high permittivity material than without it.

For a relative permittivity of 600 we also simulated cases with material electric conductivity equal to 0.35 S/m and 0.035 S/m. A conductivity of 0.35 S/m is similar to that reported for a high permittivity material previously created with a mixture of water and ceramic beads (9). Materials with relative permittivity near 600 at 128MHz consisting of solid ceramics can be produced with conductivity as low as 0.01 S/m (private communication with Sebastian Rupprecht and Michael Lanagan of the Penn State Materials Research Institute) so a conductivity of 0.035 S/m was seen as a reasonable representative of what may be possible in the future. Addition of conductivity had negligible effect on B_1 homogeneity (3D COV of 0.0988 and 0.0980 for conductivities of 0.35 S/m and 0.035 S/m, respectively), and increased normalized peak SAR by about 15% (0.0396 and 0.0350 for conductivities of 0.35 S/m and 0.035 S/m, respectively). This is still well under one half the normalized SAR with no high permittivity material present.

Discussion

A number of simulations and experiments in recent years have demonstrated a variety of potential benefits of high permittivity materials in MRI (5–10,12,13). Here we use numerical

simulations to illustrate that strategic use of these materials may reduce RF currents induced in implants not immediate to the region of interest, and thus reduce associated SAR and broaden the conditions under which patients having implants can be imaged safely.

In this example, we model a patient implanted with a pacemaker undergoing MRI of the head at 3T with a whole-body coil. MRI at 3T has become preferred over 1.5T for imaging of the brain at many sites in recent years due to its superior SNR in that region, and most receive coils for imaging the head are designed with no transmit capability, thus relying on the body coil for transmission.

With our simulations, we show the potential to reduce heating at the tip of the pacemaker by more than 40% with use of high permittivity materials surrounding the head. The thickness of 5mm was chosen as it should be thin enough to be incorporated into head-only receive array designs without significantly displacing conductive coil elements. This thickness is also consistent with simulations of receive arrays at 7T showing promising effects of high permittivity materials on receive array sensitivity (14). Nonetheless, further work would be required to examine behavior of specific receive arrays at 3T, and whether even thinner layers of high permittivity materials could have similarly beneficial effects.

Design of pacemaker leads has advanced significantly in recent years, reducing the ability of leads to carry high-frequency currents and thus reducing SAR at the tip during MRI. For example, complex winding structures in the lead are used to maximize impedance of currents at high frequencies (14). This, in part, has led to the production of pacemakers which are approved for imaging under certain conditions, or MR Conditional pacemakers. Current conditions for imaging a subject implanted with such a device include imaging at 1.5T, where SAR levels are relatively low for a given sequence compared to those at higher field strengths. We expect that the reduction of SAR demonstrated here for a simple lead with use of the high permittivity material would also result in SAR reductions for more modern leads, as the reduction of RF field strengths away from the region of interest should result in lower induced currents in a lead of any design. Our results demonstrate that strategic use of high permittivity materials may be useful in allowing for MRI of subjects with pacemakers at 3T, which is often preferred over 1.5T for imaging of the brain.

There are challenges to implementation of an HPM helmet like that proposed here. While thicker layers of lower permittivity materials have been used to enhance fields around the heart and head at 3T, the use of these lower permittivities requires more material, which could impede placement of a receive array near the head. Flexible materials with relative permittivities up to about 515 at 3T have been produced by mixing water with powder (15) or beads (9) of various high-permittivity ceramics. For routine use of HPM materials, though, solid materials integrated into receive arrays may be preferable. With solid ceramics, it is possible to achieve relative permittivities greater than 1000. Cost of manufacturing such materials in thin anatomically-conforming shapes, however, warrant further study before implementation, including design of a receive array incorporating the material and considering effects of the relative permittivity on receive performance.

Importantly, because the potential benefits predicted here regarding safety of subjects with active implanted devices have been investigated only with numerical simulations at this time, it is necessary that these results be validated experimentally in phantoms with realistic devices and with consideration of the stringent requirements for determining conditions for safely imaging a subject having such an implant (16) before any attempt to apply these concepts in vivo.

Acknowledgments

Funding: NIH P41 EB017183, NIH R01 EB006563, NSFC 61172034 and NSFC 61528102

References

1. Nazarian S, Beinart R, Halperin HR. Magnetic Resonance Imaging and Implantable Devices. Circ-Arrhythmia Elec. 2013; 6(2):419–428.
2. Shellock FG, Kanal E. Policies, Guidelines, and Recommendations for Mr Imaging Safety and Patient-Management. Jmri-J Magn Reson Im. 1991; 1(1):97–101.
3. Levine GN, Gomes AS, Arai AE, Bluemke DA, Flamm SD, Kanal E, Manning WJ, Martin ET, Smith JM, Wilke N, Shellock FS. Safety of magnetic resonance imaging in patients with cardiovascular devices - An American Heart Association scientific statement from the committee on diagnostic and interventional cardiac catheterization, council on clinical cardiology, and the council on cardiovascular radiology and intervention. Circulation. 2007; 116(24):2878–2891. [PubMed: 18025533]
4. Nordbeck P, Ertl G, Ritter O. Magnetic resonance imaging safety in pacemaker and implantable cardioverter defibrillator patients: how far have we come? Eur Heart J. 2015; 36(24):1505–U1581. [PubMed: 25796053]
5. Yang QX, Rupprecht S, Luo W, Sica C, Herse Z, Wang JL, Cao ZP, Vesek J, Lanagan MT, Carluccio G, Ryu YC, Collins CM. Radiofrequency field enhancement with high dielectric constant (HDC) pads in a receive array coil at 3.0T. J Magn Reson Imaging. 2013; 38(2):435–440. [PubMed: 23293090]
6. Brink WM, Webb AG. High Permittivity Pads Reduce Specific Absorption Rate, Improve B-1 Homogeneity, and Increase Contrast-to-Noise Ratio for Functional Cardiac MRI at 3 T. Magn Reson Med. 2014; 71(4):1632–1640. [PubMed: 23661547]
7. de Heer P, Brink WM, Kooij BJ, Webb AG. Increasing signal homogeneity and image quality in abdominal imaging at 3 T with very high permittivity materials. Magn Reson Med. 2012; 68(4): 1317–1324. [PubMed: 22851426]
8. Lindley MD, Kim D, Morrell G, Heilbrun ME, Storey P, Hanrahan CJ, Lee VS. High-Permittivity Thin Dielectric Padding Improves Fresh Blood Imaging of Femoral Arteries at 3 T. Investigative Radiology. 2015; 50(2):101–107. [PubMed: 25329606]
9. Luo W, Lanagan MT, Sica CT, Ryu Y, Oh S, Ketterman M, Yang QX, Collins CM. Permittivity and performance of dielectric pads with sintered ceramic beads in MRI: early experiments and simulations at 3 T. Magn Reson Med. 2013; 70(1):269–275. [PubMed: 22890908]
10. Yang QX, Wang JL, Wang JH, Collins CM, Wang CS, Smith MB. Reducing SAR and Enhancing Cerebral Signal-to-Noise Ratio with High Permittivity Padding at 3 T. Magn Reson Med. 2011; 65(2):358–362. [PubMed: 21264928]
11. Christ A, Kainz W, Hahn EG, Honegger K, Zefferer M, Neufeld E, Rascher W, Janka R, Bautz W, Chen J, Kiefer B, Schmitt P, Hollenbach HP, Shen JX, Oberle M, Szczerba D, Kam A, Guag JW, Kuster N. The Virtual Family-development of surface-based anatomical models of two adults and two children for dosimetric simulations. Phys Med Biol. 2010; 55(2):N23–N38. [PubMed: 20019402]
12. Webb AG. Dielectric Materials in Magnetic Resonance. Concept Magn Reson A. 2011; 38a(4): 148–184.

13. Yang QX, Mao WH, Wang JH, Smith MB, Lei H, Zhang XL, Ugurbil K, Chen W. Manipulation of image intensity distribution at 7.0 T: Passive RF shimming and focusing with dielectric materials. J Magn Reson Imaging. 2006; 24(1):197–202. [PubMed: 16755543]

14. Gray RW, Bibens WT, Shellock FG. Simple design changes to wires to substantially reduce MRI-induced heating at 1.5 T: implications for implanted leads. Magn Reson Imaging. 2005; 23(8): 887–891. [PubMed: 16275428]

15. Haines K, Smith NB, Webb AG. New high dielectric constant materials for tailoring the B-1(+) distribution at high magnetic fields. J Magn Reson. 2010; 203(2):323–327. [PubMed: 20122862]

16. ISO/TS 10974:2012(E). Assessment of the safety of magnetic resonance imaging for patients with an active implantable medical device. Geneva: International Organization for Standardization; 2012.

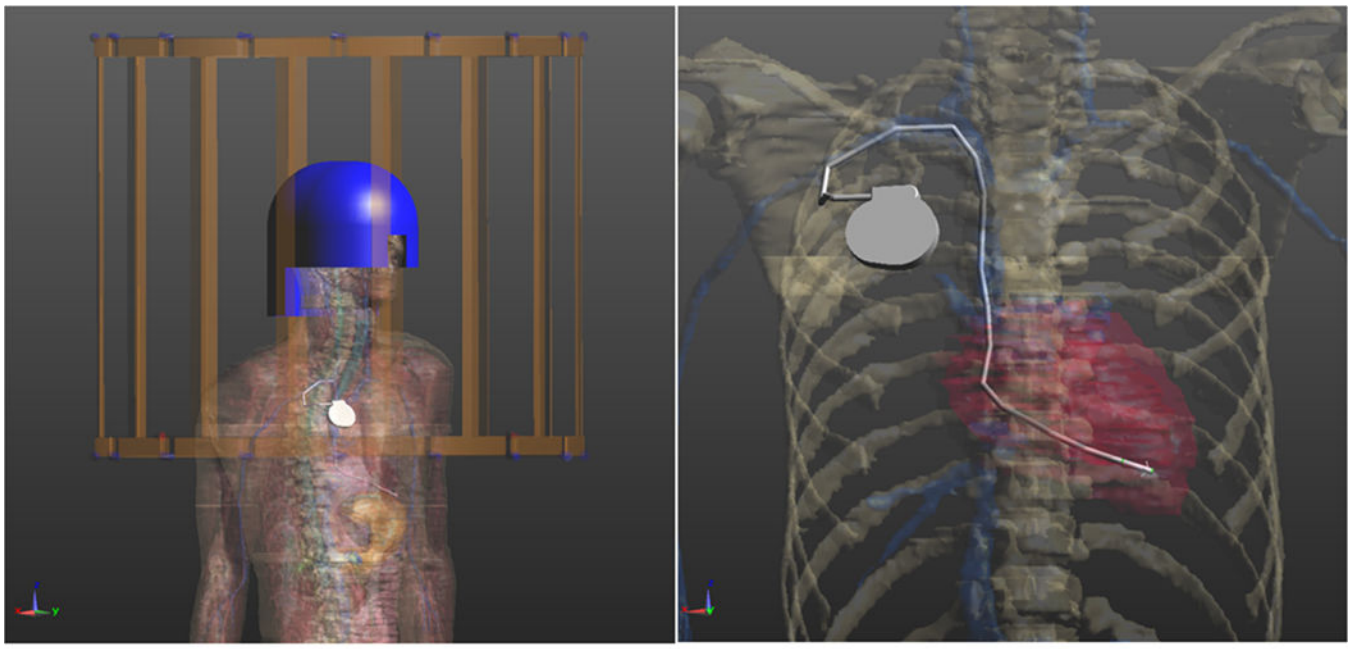

(a) (b)

Fig. 1.

Geometry of the CAD model: (a) Numerical model of body birdcage coil (gold) loaded with human model “Duke” with high-dielectric head coil former (blue) and pacemaker with implanted lead (silver); (b) Portion of problem geometry showing pacemaker.

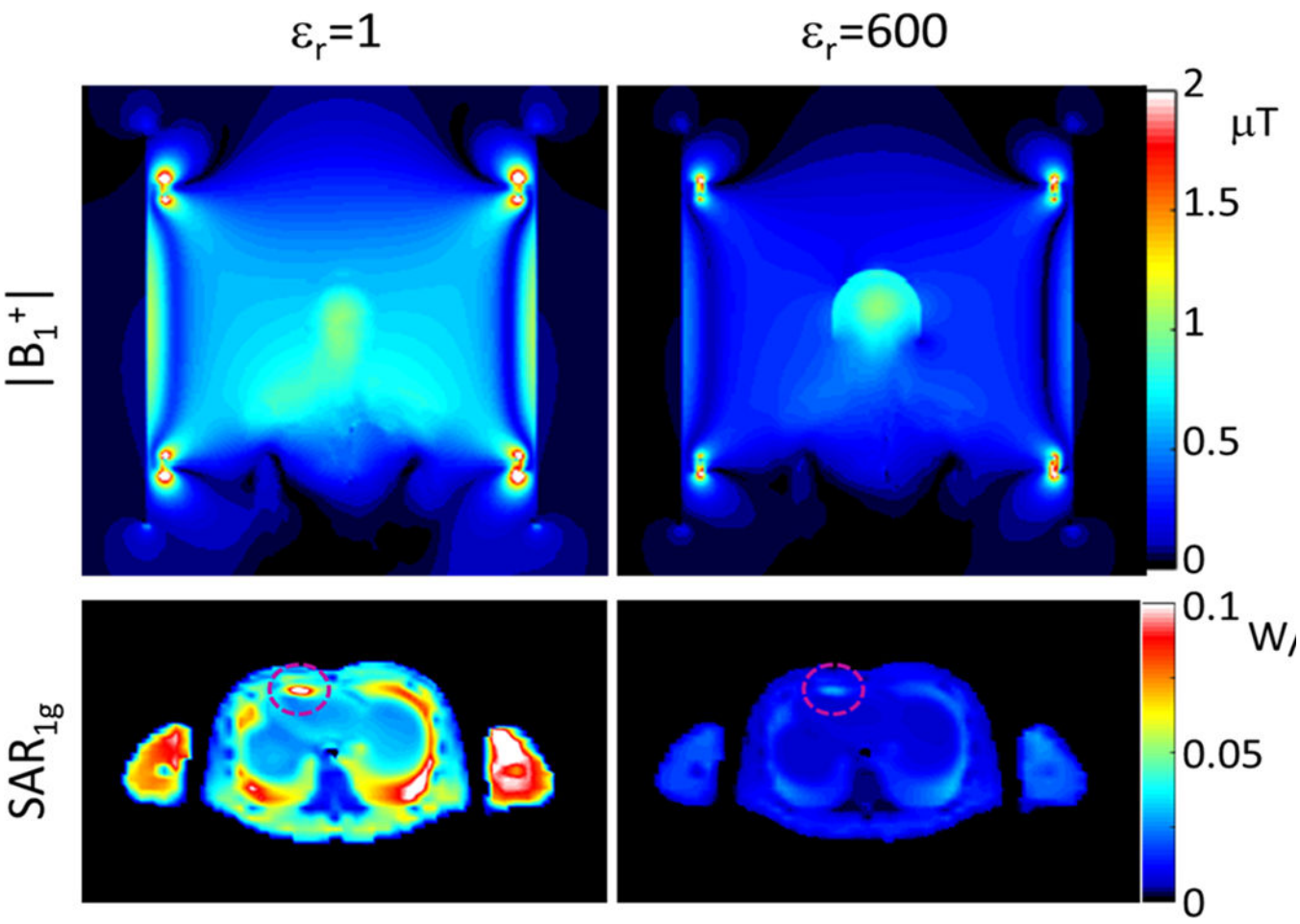

Fig. 2.

Distributions of B_1 field (top) and SAR_{1g} (bottom) for an excitation with the body coil driven to produce 1 μT at the center of brain without (left) or with (right) a 5mm-thick shell having a relative electric permittivity of 600 surrounding the head of the subject.

Table 1

Results of head coil former on SAR_{1g} around the implanted lead tips and B_1 field homogeneity on the mid-transverse slice in brain as well as in the entire cerebrum with the body coil driven to produce a 1μT B_1^+ field at the center of brain.

Relative permittivity of the head coil former	Peak SAR/|B1+|^2 W/kg/(μT)^2	Coefficient of Variation of |B1+| on transverse plane	Coefficient of Variation of |B1+| in cerebrum
1	0.1153	0.0763	0.1408
300	0.0717	0.0738	0.1092
400	0.0530	0.0697	0.1076
500	0.0392	0.0688	0.1053
600	0.0306	0.0665	0.0981
700	0.0229	0.0683	0.1041
900	0.0152	0.0692	0.1208